Accurate predictions for charged Higgs production: Closing the $m_{H^\pm} \sim m_t$ window

Céline Degrande [a], Rikkert Frederix [b], Valentin Hirschi [c], Maria Ubiali [d,*], Marius Wiesemann [e], Marco Zaro [f,g]

[a] *Institute for Particle Physics Phenomenology, Department of Physics, Durham University, Durham DH1 3LE, United Kingdom*
[b] *Technische Universität München, James-Franck-Str. 1, D-85748 Garching, Germany*
[c] *SLAC, National Accelerator Laboratory, 2575 Sand Hill Road, Menlo Park, CA 94025-7090, USA*
[d] *Cavendish Laboratory, HEP group, University of Cambridge, J.J. Thomson Avenue, Cambridge CB3 0HE, United Kingdom*
[e] *Physik-Institut, Universität Zürich, Winterthurerstr. 190, 8057 Zurich, Switzerland*
[f] *Sorbonne Universités, UPMC Univ. Paris 06, UMR 7589, LPTHE, F-75005, Paris, France*
[g] *CNRS, UMR 7589, LPTHE, F-75005, Paris, France*

ARTICLE INFO

ABSTRACT

We present predictions for the total cross section for the production of a charged Higgs boson in the intermediate-mass range ($m_{H^\pm} \sim m_t$) at the LHC, focusing on a type-II two-Higgs-doublet model. Results are obtained at next-to-leading order (NLO) accuracy in QCD perturbation theory, by studying the full process $pp \to H^\pm W^\mp b\bar{b}$ in the complex-(top)-mass scheme with massive bottom quarks. Compared to lowest-order predictions, NLO corrections have a sizeable impact: they increase the cross section by roughly 50% and reduce uncertainties due to scale variations by more than a factor of two. Our computation reliably interpolates between the low- and high-mass regime. Our results provide the first NLO prediction for charged Higgs production in the intermediate-mass range and therefore allow to have NLO accurate predictions in the full $m_{H^\pm}$ range. The extension of our results to different realisations of the two-Higgs-doublet model or to the supersymmetric case is also discussed.

Charged Higgs bosons appear in the scalar sector of several Standard Model (SM) extensions, and are the object of various beyond the Standard Model (BSM) searches at the LHC. As the SM does not include any elementary charged scalar particle, the observation of a charged Higgs boson would necessarily point to a non-trivially extended scalar sector.

In this paper we focus on a generic two-Higgs-doublet model (2HDM), which is one of the simplest SM extensions featuring a charged scalar. Within this class of models, two isospin doublets are introduced to break the $SU(2) \times U(1)$ symmetry, leading to the existence of five physical Higgs bosons, two of which are charged particles ($H^\pm$). Imposing flavour conservation, there are four possible ways to couple the SM fermions to the two Higgs

doublets [1]. Each of the four ways gives rise to rather different phenomenologies. In this work, we consider the so-called type-II 2HDM (although we will discuss how our results can be generalised to other types), in which one doublet couples to up-type quarks and the other to down-type quarks and charged leptons.

The dominant production mode for a charged Higgs boson depends on the value of its mass with respect to the top-quark mass, and can be classified into three categories. Light charged Higgs scenarios are defined by Higgs-boson masses smaller than the mass of the top quark, where the top-quark decay $t \to H^+ b$ is allowed and the charged Higgs is light enough so that top-quark off-shell effects can be neglected (typically experimental analyses consider masses up to $m_{H^\pm} \lesssim 160$ GeV). The cross section for the production of a light charged Higgs boson is simply given by the product of the top-pair production cross section and the branching ratio of a top quark into a charged Higgs boson, see Fig. 1 (a). The former is known up to next-to-next-to-leading order in perturbative QCD [2] and displays a 3% QCD scale uncertainty, while the NLO branching ratio for $t \to H^+ b$ [3–13] is affected by a 2% scale uncertainty due to missing higher-order QCD contributions. Thus the theoretical ac-

* Corresponding author.
E-mail addresses: celine.degrande@durham.ac.uk (C. Degrande), rikkert.frederix@tum.de (R. Frederix), vahirsch@slac.stanford.edu (V. Hirschi), ubiali@hep.phy.cam.ac.uk (M. Ubiali), mariusw@physik.uzh.ch (M. Wiesemann), zaro@lpthe.jussieu.fr (M. Zaro).
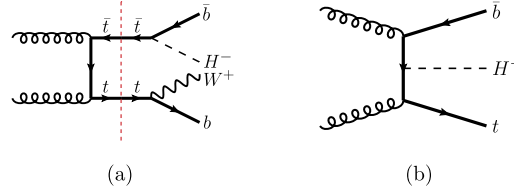
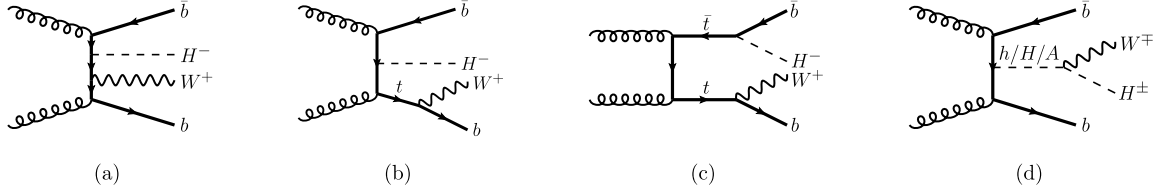**Fig. 1.** Sample LO diagrams for (a) light and (b) heavy charged Higgs production.

Fig. 2. Sample LO diagrams for the full $pp \to H^{\pm}W^{\mp}b\bar{b}$ process: (a) non-resonant top-quark contribution; (b) single-resonant top-quark contribution; (c) double-resonant top-quark contribution; (d) contribution involving neutral scalars.

curacy for the production of a light charged Higgs boson is at the few % level. The model-independent bounds on the branching ratio of a light charged Higgs boson [14] are transformed into limits in the $(m_{H^{\pm}}, \tan\beta)$ plane, with $\tan\beta$ being the ratio of the vacuum expectation values of the two Higgs doublets. Direct searches at the LHC, with a centre-of-mass energy of 7 TeV [15–18] and 8 TeV [19,20] set stringent constraints on the parameter space with a light charged Higgs boson.

Heavy charged Higgs boson scenarios, on the other hand, correspond to charged Higgs masses larger than the top-quark mass (typically $m_{H^{\pm}} \gtrsim 200$ GeV). In this case, the dominant charged Higgs production channel is the associated production with a top quark,[1] see Fig. 1(b). Theoretical predictions at NLO(+PS) have been computed both at the inclusive and fully-differential level in the five-flavour scheme (5FS) [21–28] and in the four-flavour scheme (4FS) [29,30,28]. Charged Higgs searches at 7 TeV [15], 8 TeV [31,32,20] and 13 TeV [33–35] have set upper limits on the cross section for heavy charged Higgs production times branching ratio BR($H^{\pm} \to \tau\nu_{\tau}$) for charged Higgs-boson masses ranging from 200 to 2000 GeV.

The intermediate-mass range is associated with charged Higgs masses close to the top-quark mass ($145 \lesssim m_{H^{\pm}} \lesssim 200$ GeV). In this region, finite top-width effects as well as the interplay between top-quark resonant and non-resonant diagrams cannot be neglected. Therefore, the full process $pp \to H^{\pm}W^{\mp}b\bar{b}$ (with massive bottom quarks), see Fig. 2, including non-resonant, single-resonant and double-resonant contributions, has to be considered, to perform a reliable perturbative computation of the charged Higgs cross section. The intermediate-mass range has not been searched for at the LHC to date, mostly due to the lack of sufficiently accurate theoretical predictions, and the consequent shortage of specific strategies devised to increase the sensitivity to the signal. Despite the fact that some studies exist on the intermediate mass-range, they are either only LO-accurate, thus affected by large theoretical uncertainties [36–38], or based on an incoherent sum of the $pp \to t\bar{t}$ and $pp \to tH^{-}$ production mechanisms [24,27], and neglecting interferences between the two. With this work, where we compute the cross section for the $pp \to H^{\pm}W^{\mp}b\bar{b}$ process at NLO accuracy, we provide for the first time precise and theoretically consistent predictions in the intermediate-mass range, which are an essential ingredient for $H^{\pm}$ searches at Run II of the LHC. We leave it to further work in collaboration with our experimental

colleagues to devise appropriate cuts and selection strategies that would maximise the sensitivity to this particular mass range. Despite the fact that indirect exclusion bounds from flavour physics for a type-II Higgs doublet model are now very strong and exclude charged Higgs boson lighter than 380 GeV,[2] the intermediate-mass region is not excluded for type-I models nor for models that embed the 2HDM-II at tree-level. Indeed, the intermediate-mass range has recently gained extra attention in the model-building community. For example, supersymmetric scenarios where the heavy Higgs boson of the spectrum has a mass of 125 GeV and the light Higgs can possibly act as a mediator to the dark-matter sector lead to a charged Higgs-boson mass similar to the top-quark mass [43, 44]. In fact, at tree-level, the Higgs-fermion Yukawa couplings of the MSSM and p-MSSM follow the 2HDM-II pattern. However, when radiative corrections are included, the Yukawa couplings are modified by supersymmetry-breaking effects, thus leading to a different phenomenology. It is important to notice that such modifications of the Yukawa coupling can be included in our calculation, as it is explicitly spelled out in the following.

Our computation employs a chain of automatic tools in the MadGraph5_aMC@NLO + NLOCT framework [45,46], developed to study the phenomenology of new physics models at NLO accuracy. In this framework, NLOCT automatically computes the R_2 rational terms and the ultraviolet counterterms used in the virtual amplitudes, and relies internally upon FeynRules [47] and FeynArts [48]. The one-loop matrix elements are computed using the MadLoop module [49], which employs CutTools [50] and Ninja [51–53] for loop reduction at the integrand level and IREGI [54] for tensor integral reduction. All methods are complemented by an in-house implementation of the OpenLoops [55] algorithm. For the factorisation of the IR poles in the real-emission phase-space integrals, the resonance-aware MadFKS [56,57] module is used.

We work in the four-flavour scheme, where the bottom-quark mass regulates any soft or collinear divergence related to final-state bottom-quark emissions, making it possible to compute the total cross section without having to impose artificial cuts on the final state particles. In a 5FS version of this computation ($b\bar{b} \to H^{\pm}W^{\mp}$), non-, single- and double-resonant contributions are included at different accuracies. In particular the double-resonant contributions only enter at NNLO (and beyond). Even in that case, these contributions would be effectively included only at lowest

---

[1] In the four-flavour scheme there is also an explicit bottom quark in the final state.

[2] See e.g. refs. [39–42].

Table 1

LO and NLO total cross sections (in pb) and K-factors for the $pp \to H^+ W^- b\bar{b}$ process, for $\tan\beta = 1, 8, 30$ at the 13 TeV LHC. The first quoted uncertainties are from scale variations, the second from PDFs (both in per cent of the total cross section). The statistical uncertainty from the numerical phase-space integration is of the order of 1% or below.

$m_{H^\pm}$ [GeV]	$\tan\beta = 1$			$\tan\beta = 8$			$\tan\beta = 30$		
	σ_{LO}	σ_{NLO}	K	σ_{LO}	σ_{NLO}	K	σ_{LO}	σ_{NLO}	K
145	$47.8^{+31}_{-22} \pm 2.4$	$71.6^{+7}_{-9} \pm 2.4$	1.50	$2.17^{+39}_{-26} \pm 2.4$	$3.26^{+8}_{-11} \pm 2.4$	1.50	$13.5^{+46}_{-29} \pm 2.4$	$21.0^{+10}_{-14} \pm 2.5$	1.55
150	$35.7^{+31}_{-22} \pm 2.4$	$53.1^{+7}_{-9} \pm 2.4$	1.49	$1.57^{+39}_{-26} \pm 2.4$	$2.38^{+8}_{-12} \pm 2.4$	1.52	$9.81^{+46}_{-29} \pm 2.4$	$15.1^{+10}_{-14} \pm 2.4$	1.54
155	$24.1^{+31}_{-22} \pm 2.4$	$36.3^{+7}_{-10} \pm 2.4$	1.51	$1.04^{+39}_{-26} \pm 2.4$	$1.61^{+8}_{-12} \pm 2.4$	1.54	$6.34^{+46}_{-29} \pm 2.4$	$9.99^{+10}_{-14} \pm 2.4$	1.58
160	$14.1^{+31}_{-22} \pm 2.5$	$21.6^{+8}_{-10} \pm 2.5$	1.53	$0.609^{+39}_{-26} \pm 2.4$	$0.943^{+9}_{-12} \pm 2.5$	1.55	$3.64^{+47}_{-29} \pm 2.5$	$5.85^{+11}_{-15} \pm 2.5$	1.60
165	$6.50^{+32}_{-23} \pm 2.6$	$10.1^{+9}_{-11} \pm 2.6$	1.56	$0.274^{+40}_{-26} \pm 2.5$	$0.442^{+11}_{-14} \pm 2.5$	1.61	$1.68^{+48}_{-30} \pm 2.6$	$2.72^{+13}_{-16} \pm 2.6$	1.62
170	$2.95^{+34}_{-23} \pm 2.9$	$4.51^{+10}_{-12} \pm 3.0$	1.53	$0.095^{+43}_{-27} \pm 2.9$	$0.149^{+13}_{-15} \pm 3.0$	1.56	$0.763^{+50}_{-31} \pm 3.0$	$1.20^{+14}_{-17} \pm 3.0$	1.58
175	$2.60^{+34}_{-28} \pm 3.0$	$3.98^{+10}_{-12} \pm 3.0$	1.53	$0.083^{+43}_{-28} \pm 3.0$	$0.131^{+13}_{-15} \pm 3.0$	1.58	$0.674^{+51}_{-31} \pm 3.1$	$1.07^{+14}_{-17} \pm 3.1$	1.59
180	$2.41^{+34}_{-28} \pm 3.1$	$3.71^{+10}_{-12} \pm 3.1$	1.54	$0.077^{+44}_{-28} \pm 3.1$	$0.121^{+13}_{-15} \pm 3.2$	1.59	$0.627^{+51}_{-31} \pm 3.1$	$0.998^{+14}_{-17} \pm 3.2$	1.59
185	$2.27^{+35}_{-24} \pm 3.1$	$3.51^{+10}_{-12} \pm 3.1$	1.55	$0.073^{+44}_{-28} \pm 3.1$	$0.115^{+13}_{-15} \pm 3.1$	1.59	$0.591^{+51}_{-32} \pm 3.2$	$0.947^{+15}_{-17} \pm 3.2$	1.60
190	$2.15^{+35}_{-24} \pm 3.1$	$3.32^{+10}_{-12} \pm 3.2$	1.54	$0.069^{+44}_{-28} \pm 3.2$	$0.109^{+13}_{-15} \pm 3.2$	1.58	$0.561^{+51}_{-32} \pm 3.2$	$0.896^{+14}_{-17} \pm 3.3$	1.60
195	$2.05^{+35}_{-24} \pm 3.2$	$3.18^{+11}_{-12} \pm 3.2$	1.56	$0.066^{+44}_{-28} \pm 3.2$	$0.105^{+13}_{-15} \pm 3.2$	1.60	$0.536^{+52}_{-32} \pm 3.2$	$0.850^{+14}_{-17} \pm 3.2$	1.59
200	$1.95^{+35}_{-24} \pm 3.2$	$3.02^{+10}_{-12} \pm 3.3$	1.55	$0.063^{+44}_{-28} \pm 3.2$	$0.100^{+13}_{-15} \pm 3.3$	1.58	$0.510^{+52}_{-32} \pm 3.3$	$0.812^{+14}_{-17} \pm 3.3$	1.59

order, hampering the formal accuracy of the computation in the region $m_{H^\pm} < m_t$, where they are dominant. On the other hand, in our 4FS calculation all contributions are included at NLO accuracy. Moreover, the 4FS has been shown to provide reliable predictions for the heavy-Higgs case [29,28], without being spoiled by large logarithms. For consistency, we use the four-flavour set of the PDF4LHC15 parton distributions [58–61], and the corresponding running of α_s with $\alpha_s(m_Z) = 0.1126$.

The identification of the hard scales in a complex process, such as the one at hand, is not necessarily a trivial task. One has to bear in mind, however, that in the intermediate region it is desirable to have a matching to the scale in the $pp \to t\bar{t}$ cross section for light charged Higgs masses, where the natural choice is of the order of the top-quark mass (or below [62]), and for larger masses to the scale in the heavy charged Higgs cross section, where the scale $\mu = (m_t + m_{H^\pm} + m_b)/3$ is typically applied in 4FS computations. We therefore fix our renormalisation and factorisation scales (μ_r and μ_f) to $\mu = 125$ GeV, which matches the numerical value used for the heavy charged Higgs production at $m_{H^\pm} = 200$ GeV, while it satisfies the requirement of being in between $m_t/2$ and m_t for the light charged-Higgs case.

The top-quark mass and Yukawa coupling are renormalized on-shell, while we use a hybrid scheme for the bottom-quark mass: kinematical bottom-quark masses are treated with an on-shell renormalization, but the $\overline{\mathrm{MS}}$ renormalisation scheme is employed for the bottom-quark Yukawa coupling. For the numerical values we follow the recommendations of the LHC Higgs Cross Section Working Group [63], which implies $m_t^{\mathrm{OS}} = 172.5$ GeV and $m_b^{\mathrm{OS}} = 4.92$ GeV for the on-shell masses. Using the four-loop conversion [64] and running, this corresponds to the $\overline{\mathrm{MS}}$ bottom mass $m_b(m_b) \simeq 4.18$ GeV and $m_b(\mu) \simeq 2.81$ GeV, respectively. For the computation of scale variations starting from $m_b(\mu)$, a two-loop running is employed.

Since the $pp \to H^\pm W^\mp b\bar{b}$ process involves resonant top-quark contributions, the width of the top quark has to be included in the computation without spoiling gauge invariance. This is achieved by employing the complex-mass scheme [65,66], where the top-quark mass (and Yukawa coupling) are regarded as complex parameters. For a given charged Higgs mass and $\tan\beta$, we compute the corresponding top-quark width at the same perturbative order in α_s as the cross section. The charged Higgs boson and the W boson are kept on-shell.

Compared to calculations of similar complexity (e.g. the $pp \to W^+W^- b\bar{b}$ process in the 4FS [67,68]), the technical challenges of this process lie in the interplay between the non-, single- and double-resonant contributions, which can have a different hierarchy depending on $m_{H^\pm}$. On top of this, the cross section receives contributions with different powers of the bottom-quark Yukawa coupling, and therefore its running cannot be accounted for through an overall factor. Unlike in previous computations [69, 28] these contributions, including scale variations, are computed simultaneously.

Among the various Feynman diagrams contributing to the $pp \to H^\pm W^\mp b\bar{b}$ process, some include the neutral Higgs states of the 2HDM (h, H, A) and their coupling to bottom quarks, see Fig. 2(d). We refrain from including these contributions in our computation at NLO, but briefly comment on the size of their effects below. To be able to make quantitative statements we must make some assumptions regarding the 2HDM parameters. We use the so-called "alignment" region ($\cos(\beta - \alpha) \simeq 0$, with α the mixing angle of the two CP even scalars), where the 125 GeV Higgs boson discovered at the LHC corresponds to the light scalar h [70].[3] In principle, m_A and m_H can be chosen such that the H and A states may become resonant. In practice, if this choice is made, one is de facto considering the simpler process $pp \to H/A b\bar{b}$, with $H/A \to H^\pm W^\mp$ decay. Therefore, we will not consider this case here. We have verified that the impact of the neutral Higgs states is completely negligible for small $\tan\beta$. At large $\tan\beta$ ($\tan\beta = 30$), we found at most -7% impact on the LO cross section for $m_{H^\pm} > 180$ GeV in the configuration $m_H = m_A \simeq m_{H^\pm} - 45$ GeV. For other values of $m_{H^\pm}$ and for heavier neutral Higgses the effect is smaller. Lighter neutral Higgses are strongly disfavoured by EW precision fits [71–73] and direct searches. We thus reckon that our choice of not including contributions from neutral Higgs bosons is justified, as their small impact can be included separately and off-line at LO without hampering the accuracy of our NLO results presented below.

We now present our results for the total cross section of the $pp \to H^+ W^- b\bar{b}$ process (the charge-conjugated process has the same total cross section) at NLO QCD, at the 13 TeV LHC. We consider three different values of the $\tan\beta$ parameter, $\tan\beta = 1, 8, 30$. The total cross sections at LO and NLO accuracy in the range $m_{H^\pm}/\mathrm{GeV} \in [145, 200]$ are given in Table 1, together with the NLO K-factors, defined as the ratio $K = \sigma_{\mathrm{NLO}}/\sigma_{\mathrm{LO}}$. Next to the total

---

[3] Models where the heavy Higgs corresponds to the particle discovered at the LHC, such as those from Ref. [44], tend to prefer small or moderate values of $\tan\beta$, which greatly suppress this kind of diagrams.
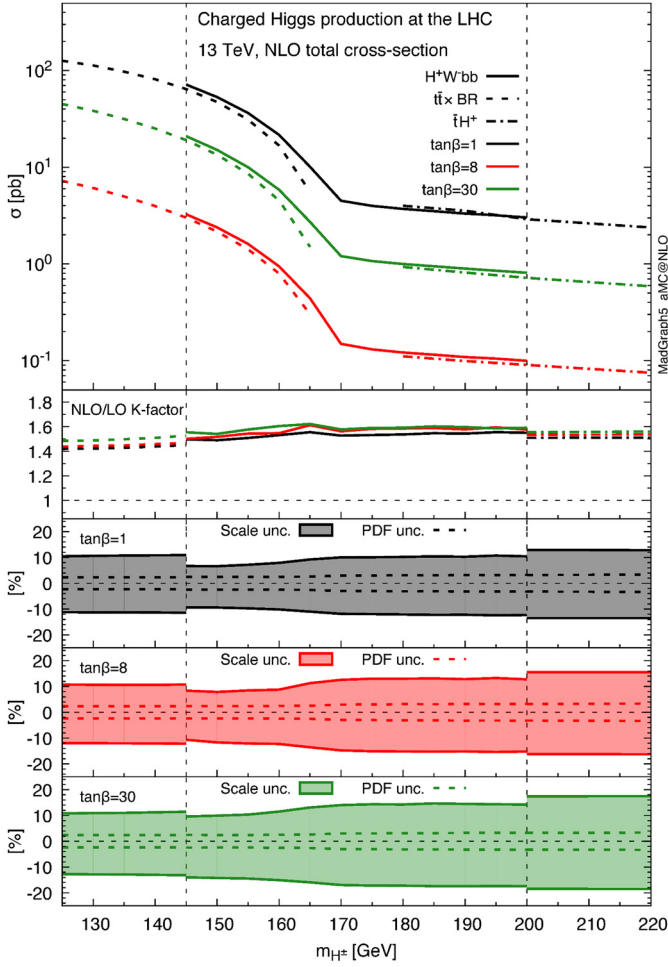
Fig. 3. NLO total cross sections, K-factors and uncertainties for charged Higgs boson production at the 13 TeV LHC. (For interpretation of the references to colour in this figure legend, the reader is referred to the web version of this article.)

cross sections, we quote the scale and PDF uncertainties. Scale uncertainties are computed by varying independently the renormalisation and factorisation scales in the range $\mu_r, \mu_f \in [\mu/2, 2\mu]$ (albeit keeping the scale in the computation of the top-quark width fixed to the central value), while for PDF uncertainties we follow the PDF4LHC15 procedure [58]. NLO corrections are large; they increase the central value of the total cross section by 50%–60%, with only a very mild dependence on the charged Higgs-boson mass and $\tan\beta$ value, and significantly reduce the scale dependence with respect to LO. More precisely, NLO scale uncertainties range between 8%–13% (10%–17%) for $m_{H^\pm} < m_t$ ($m_{H^\pm} > m_t$). In both cases, the large-$\tan\beta$ ($\sigma \sim y_b^2$) scenario features larger scale uncertainties than the small-$\tan\beta$ ($\sigma \sim y_t^2$) one, because of the additional μ_r-dependence introduced by the running of the bottom-quark Yukawa coupling.

Further details on the behaviour of the scale uncertainties can be inferred from Fig. 3, where we compare our intermediate-mass range results to dedicated predictions for light and heavy charged Higgs production. The input parameters have been chosen consistently across all the mass range, in particular all cross sections are computed in the 4FS, the central scale for low-mass range is also set to $\mu = 125$ GeV, while the scale $\mu = (m_t + m_{H^\pm} + m_b)/3$ is used for the heavy charged Higgs case. The central predictions in the main frame develop a prominent structure with a kink at the threshold $m_{H^\pm} \simeq m_t - m_b$. The effect of the single-resonant contributions ($pp \to tW^-$ and $pp \to \bar{t}H^+$) is visible when comparing

our results in the intermediate-mass range with the low-mass prediction. Indeed, the single-resonant contributions are missing in the low-mass prediction and amount to 10%–15% of the $pp \to t\bar{t}$ cross section depending on the specific value of $\tan\beta$. In contrast, looking at the matching of the intermediate-mass predictions to the heavy charged Higgs cross section, we observe a 5%–10% gap for $\tan\beta = 8$ and $\tan\beta = 30$, while there is essentially no gap for $\tan\beta = 1$. Such a gap originates from the non-resonant part of the $pp \to H^\pm W^\mp b b$ amplitude, which, because of the chiral structure of the $H^+ tb$ and Wtb vertices, is enhanced (suppressed) for large (small) values of $\tan\beta$. At 145 and 200 GeV, the size of the scale uncertainty in the intermediate region and the side-bands is slightly different. These discontinuities are related to missing subleading terms in the predictions used in the low and high-mass regions, i.e. mostly single-resonant and non-resonant, respectively, although it is difficult to pin down exactly the origin of the discontinuities because of the non-trivial separation of these contributions beyond leading order. Finally, we note that the K-factor in the intermediate region interpolates very well the ones in the low and high-mass range.

We now discuss how to generalise our results at a single $\tan\beta$ value in order to obtain the charged Higgs boson cross section in the intermediate-mass range for any value of $\tan\beta$ or in a type-I 2HDM by means of reweighting. As discussed in Ref. [28], the cross section for charged Higgs production receives contributions proportional to y_b^2, y_t^2 and $y_b y_t$. In a type-II 2HDM, while the $y_b y_t$ contribution does not depend on $\tan\beta$, the y_b^2 and y_t^2 ones scale as $\tan\beta^2$ and $1/\tan\beta^2$, respectively. Conversely, in a type-I 2HDM, all contributions (and therefore the total cross section) scale as $1/\tan\beta^2$. We point out that a naive reweighting, such as the one proposed in Ref. [28] for a heavy charged Higgs boson, is bound to fail in our case, since it will miss effects due to the $\tan\beta$ dependence of the top width. We verified that, if the top-width dependence is included as an overall factor, we are able to reproduce our $\tan\beta = 1$ and $\tan\beta = 30$ NLO cross sections and uncertainties starting from the numbers at $\tan\beta = 8$ with an accuracy of 1% or better, using the relation (the dependence on $m_{H^\pm}$ is understood)

$$\sigma^{t-II}(\tan\beta') = \left[\left(\frac{\tan\beta'}{\tan\beta}\right)^2 \sigma^{t-II}_{y_b^2}(\tan\beta) + \sigma^{t-II}_{y_b y_t}(\tan\beta) \right.$$
$$\left. + \left(\frac{\tan\beta}{\tan\beta'}\right)^2 \sigma^{t-II}_{y_t^2}(\tan\beta) \right] \times \left(\frac{\Gamma_t(\tan\beta)}{\Gamma_t(\tan\beta')}\right)^2. \quad (1)$$

This also shows that effects due to the width-dependent complex phase of y_t are very small. Concerning how to extend our results in a type-I 2HDM, we first point out that for $\tan\beta = 1$, the cross-section is identical to the type-II case. Then, the cross-section for any other value of $\tan\beta$ can be simply obtained as

$$\sigma^{t-I}(\tan\beta') = \frac{\sigma^{t-I}(\tan\beta = 1)}{(\tan\beta')^2} \times \left(\frac{\Gamma_t(\tan\beta)}{\Gamma_t(\tan\beta')}\right)^2. \quad (2)$$

Exploiting Eqs. (1) and (2) we produced cross section tables for $\tan\beta \in [0.1, 60]$, both for a type-II and a type-I 2HDM, which are publicly available.[4] Finally, Eq. (1) can also be used to include the dominant supersymmetric corrections, in particular those which modify the relation between the bottom-quark mass and its Yukawa coupling. These corrections are enhanced at large $\tan\beta$ and can be resummed to all orders by modifying the bottom-quark Yukawa coupling [29].

---

[4] https://twiki.cern.ch/twiki/bin/view/LHCPhysics/LHCHXSWGMSSMCharged#Intermediate_mass_145_200_GeV_ch.

In conclusion, we have presented predictions for the production of an intermediate-mass charged Higgs boson. While we have focused on the case of a type-II 2HDM, our results can be easily extended to other scenarios, such as a type-I 2HDM or supersymmetry. For the first time theoretically consistent predictions at NLO QCD accuracy have been made available in this mass range. To this end, we have studied the $pp \to H^\pm W^\mp b\bar{b}$ process in the complex-mass scheme, including finite top-width effects and contributions with resonant top quarks. Our results provide a reliable interpolation of low- and high-mass regions and make it possible to finally extend direct searches for charged Higgs bosons to the $m_{H^\pm} \sim m_t$ region, so far unexplored by LHC experiments. The central value of the NLO total cross section is well-approximated by a factor of about 1.5–1.6 times the LO cross section, with only a very mild dependence on the charged Higgs mass and $\tan\beta$. The results presented in paper constitute an important step in filling a gap in the available theoretical predictions for charged Higgs boson production at next-to-leading order in QCD. Current results could be further improved by including model-dependent sub-leading contributions that may become dominant in case of large width of heavy neutral Higgses, and by considering differential distributions. We leave it to future work to study if this factorisation of the NLO corrections also holds at the same level for differential distributions, employing modern techniques developed to take into account internal resonances when matching NLO computations with parton showers [74,57,75].

Acknowledgements

References

[1] G.C. Branco, P.M. Ferreira, L. Lavoura, M.N. Rebelo, M. Sher, J.P. Silva, Theory and phenomenology of two-Higgs-doublet models, Phys. Rep. 516 (2012) 1–102, http://dx.doi.org/10.1016/j.physrep.2012.02.002, arXiv:1106.0034.

[2] M. Czakon, P. Fiedler, A. Mitov, Total top-quark pair-production cross section at hadron colliders through $O(\alpha_s^4)$, Phys. Rev. Lett. 110 (2013) 252004, http://dx.doi.org/10.1103/PhysRevLett.110.252004, arXiv:1303.6254.

[3] M. Jezabek, J.H. Kuhn, QCD corrections to semileptonic decays of heavy quarks, Nucl. Phys. B 314 (1989) 1–6, http://dx.doi.org/10.1016/0550-3213(89)90108-9.

[4] C.S. Li, R.J. Oakes, T.C. Yuan, QCD corrections to $t \to W^+ b$, Phys. Rev. D 43 (1991) 3759–3762, http://dx.doi.org/10.1103/PhysRevD.43.3759.

[5] J.M. Campbell, R.K. Ellis, F. Tramontano, Single top production and decay at next-to-leading order, Phys. Rev. D 70 (2004) 094012, http://dx.doi.org/10.1103/PhysRevD.70.094012, arXiv:hep-ph/0408158.

[6] A. Czarnecki, K. Melnikov, Two loop QCD corrections to top quark width, Nucl. Phys. B 544 (1999) 520–531, http://dx.doi.org/10.1016/S0550-3213(98)00844-X, arXiv:hep-ph/9806244.

[7] K. Chetyrkin, R. Harlander, T. Seidensticker, M. Steinhauser, Second order QCD corrections to $\Gamma(\bar{t}Wb)$, Phys. Rev. D 60 (1999) 114015, http://dx.doi.org/10.1103/PhysRevD.60.114015, arXiv:hep-ph/9906273.

[8] I.R. Blokland, A. Czarnecki, M. Slusarczyk, F. Tkachov, Heavy to light decays with a two loop accuracy, Phys. Rev. Lett. 93 (2004) 062001, http://dx.doi.org/10.1103/PhysRevLett.93.062001, arXiv:hep-ph/0403221.

[9] I.R. Blokland, A. Czarnecki, M. Slusarczyk, F. Tkachov, Next-to-next-to-leading order calculations for heavy-to-light decays, Phys. Rev. D 71 (2005) 054004, http://dx.doi.org/10.1103/PhysRevD.71.054004, arXiv:hep-ph/0503039.

[10] A. Czarnecki, J.G. Korner, J.H. Piclum, Helicity fractions of W bosons from top quark decays at NNLO in QCD, Phys. Rev. D 81 (2010) 111503, http://dx.doi.org/10.1103/PhysRevD.81.111503, arXiv:1005.2625.

[11] J. Gao, C.S. Li, H.X. Zhu, Top quark decay at next-to-next-to leading order in QCD, Phys. Rev. Lett. 110 (2013) 042001, http://dx.doi.org/10.1103/PhysRevLett.110.042001, arXiv:1210.2808.

[12] M. Brucherseifer, F. Caola, K. Melnikov, $\mathcal{O}(\alpha_s^2)$ corrections to fully-differential top quark decays, J. High Energy Phys. 1304 (2013) 059, http://dx.doi.org/10.1007/JHEP04(2013)059, arXiv:1301.7133.

[13] A. Czarnecki, S. Davidson, QCD corrections to the charged Higgs decay of a heavy quark, Phys. Rev. D 48 (1993) 4183–4187, http://dx.doi.org/10.1103/PhysRevD.48.4183, arXiv:hep-ph/9301237.

[14] O. Brein, W. Hollik, Distributions for MSSM Higgs boson + jet production at hadron colliders, Phys. Rev. D 76 (2007) 035002, http://dx.doi.org/10.1103/PhysRevD.76.035002, arXiv:0705.2744.

[15] G. Aad, et al., Search for charged Higgs bosons decaying via $H^+ \to \tau\nu$ in top quark pair events using pp collision data at $\sqrt{s} = 7$ TeV with the ATLAS detector, J. High Energy Phys. 06 (2012) 039, http://dx.doi.org/10.1007/JHEP06(2012)039, arXiv:1204.2760.

[16] G. Aad, et al., Search for charged Higgs bosons through the violation of lepton universality in $t\bar{t}$ events using pp collision data at $\sqrt{s} = 7$ TeV with the ATLAS experiment, J. High Energy Phys. 03 (2013) 076, http://dx.doi.org/10.1007/JHEP03(2013)076, arXiv:1212.3572.

[17] G. Aad, et al., Search for a light charged Higgs boson in the decay channel $H^+ \to c\bar{s}$ in $t\bar{t}$ events using pp collisions at $\sqrt{s} = 7$ TeV with the ATLAS detector, Eur. Phys. J. C 73 (6) (2013) 2465, http://dx.doi.org/10.1140/epjc/s10052-013-2465-z, arXiv:1302.3694.

[18] S. Chatrchyan, et al., Search for a light charged Higgs boson in top quark decays in pp collisions at $\sqrt{s} = 7$ TeV, J. High Energy Phys. 07 (2012) 143, http://dx.doi.org/10.1007/JHEP07(2012)143, arXiv:1205.5736.

[19] V. Khachatryan, et al., Search for a light charged Higgs boson decaying to $c\bar{s}$ in pp collisions at $\sqrt{s} = 8$ TeV, J. High Energy Phys. 12 (2015) 178, http://dx.doi.org/10.1007/JHEP12(2015)178, arXiv:1510.04252.

[20] V. Khachatryan, et al., Search for a charged Higgs boson in pp collisions at $\sqrt{s} = 8$ TeV, J. High Energy Phys. 11 (2015) 018, http://dx.doi.org/10.1007/JHEP11(2015)018, arXiv:1508.07774.

[21] S.-h. Zhu, Complete next-to-leading order QCD corrections to charged Higgs boson associated production with top quark at the CERN large hadron collider, Phys. Rev. D 67 (2003) 075006, http://dx.doi.org/10.1103/PhysRevD.67.075006, arXiv:hep-ph/0112109.

[22] G. Gao, G. Lu, Z. Xiong, J. Yang, Loop effects and nondecoupling property of SUSY QCD in $gb \to tH$, Phys. Rev. D 66 (2002) 015007, http://dx.doi.org/10.1103/PhysRevD.66.015007, arXiv:hep-ph/0202016.

[23] T. Plehn, Charged Higgs boson production in bottom gluon fusion, Phys. Rev. D 67 (2003) 014018, http://dx.doi.org/10.1103/PhysRevD.67.014018, arXiv:hep-ph/0206121.

[24] E.L. Berger, T. Han, J. Jiang, T. Plehn, Associated production of a top quark and a charged Higgs boson, Phys. Rev. D 71 (2005) 115012, http://dx.doi.org/10.1103/PhysRevD.71.115012, arXiv:hep-ph/0312286.

[25] N. Kidonakis, Charged Higgs production: higher-order corrections, PoS HEP2005 (2006) 336, arXiv:hep-ph/0511235.

[26] C. Weydert, S. Frixione, M. Herquet, M. Klasen, E. Laenen, T. Plehn, G. Stavenga, C.D. White, Charged Higgs boson production in association with a top quark in MC@NLO, Eur. Phys. J. C 67 (2010) 617–636, http://dx.doi.org/10.1140/epjc/s10052-010-1320-8, arXiv:0912.3430.

[27] M. Klasen, K. Kovarik, P. Nason, C. Weydert, Associated production of charged Higgs bosons and top quarks with POWHEG, Eur. Phys. J. C 72 (2012) 2088, http://dx.doi.org/10.1140/epjc/s10052-012-2088-9, arXiv:1203.1341.

[28] C. Degrande, M. Ubiali, M. Wiesemann, M. Zaro, Heavy charged Higgs boson production at the LHC, J. High Energy Phys. 10 (2015) 145, http://dx.doi.org/10.1007/JHEP10(2015)145, arXiv:1507.02549.

[29] S. Dittmaier, M. Kramer, M. Spira, M. Walser, Charged-Higgs-boson production at the LHC: NLO supersymmetric QCD corrections, Phys. Rev. D 83 (2011) 055005, http://dx.doi.org/10.1103/PhysRevD.83.055005, arXiv:0906.2648.

[30] M. Flechl, R. Klees, M. Kramer, M. Spira, M. Ubiali, Improved cross-section predictions for heavy charged Higgs boson production at the LHC, Phys. Rev. D 91 (7) (2015) 075015, http://dx.doi.org/10.1103/PhysRevD.91.075015, arXiv:1409.5615.

[31] G. Aad, et al., Search for charged Higgs bosons in the $H^{\pm} \to tb$ decay channel in pp collisions at $\sqrt{s} = 8$ TeV using the ATLAS detector, J. High Energy Phys. 03 (2016) 127, http://dx.doi.org/10.1007/JHEP03(2016)127, arXiv:1512.03704.

[32] G. Aad, et al., Search for charged Higgs bosons decaying via $H^{\pm} \to \tau^{\pm}\nu$ in fully hadronic final states using pp collision data at $\sqrt{s} = 8$ TeV with the ATLAS detector, J. High Energy Phys. 03 (2015) 088, http://dx.doi.org/10.1007/JHEP03(2015)088, arXiv:1412.6663.

[33] M. Aaboud, et al., Search for charged Higgs bosons produced in association with a top quark and decaying via $H^{\pm} \to \tau\nu$ using pp collision data recorded at $\sqrt{s} = 13$ TeV by the ATLAS detector, Phys. Lett. B 759 (2016) 555–574, http://dx.doi.org/10.1016/j.physletb.2016.06.017, arXiv:1603.09203.

[34] ATLAS collaboration, Search for charged Higgs bosons in the τ + jets final state using 14.7 fb^{-1} of pp collision data, recorded at $\sqrt{s} = 13$ TeV with the ATLAS experiment.

[35] ATLAS collaboration, Search for charged Higgs bosons in the $H^{\pm} \to tb$ decay channel in pp collisions at $\sqrt{s} = 13$ TeV using the ATLAS detector.

[36] S. Moretti, K. Odagiri, P. Richardson, M.H. Seymour, B.R. Webber, Implementation of supersymmetric processes in the HERWIG event generator, J. High Energy Phys. 04 (2002) 028, http://dx.doi.org/10.1088/1126-6708/2002/04/028, arXiv:hep-ph/0204123.

[37] K.A. Assamagan, M. Guchait, S. Moretti, Charged Higgs bosons in the transition region $M_{H^{\pm}} \sim m_t$ at the LHC, in: Physics at TeV colliders, Proceedings, Workshop, Les Houches, France, May 26–June 3, 2003, 2004, arXiv:hep-ph/0402057.

[38] J. Alwall, J. Rathsman, Improved description of charged Higgs boson production at hadron colliders, J. High Energy Phys. 12 (2004) 050, http://dx.doi.org/10.1088/1126-6708/2004/12/050, arXiv:hep-ph/0409094.

[39] O. Deschamps, S. Descotes-Genon, S. Monteil, V. Niess, S. T'Jampens, V. Tisserand, The two Higgs doublet of type II facing flavour physics data, Phys. Rev. D 82 (2010) 073012, http://dx.doi.org/10.1103/PhysRevD.82.073012, arXiv:0907.5135.

[40] A. Broggio, E.J. Chun, M. Passera, K.M. Patel, S.K. Vempati, Limiting two-Higgs-doublet models, J. High Energy Phys. 11 (2014) 058, http://dx.doi.org/10.1007/JHEP11(2014)058, arXiv:1409.3199.

[41] D. Das, New limits on tan β for 2HDMs with Z_2 symmetry, Int. J. Mod. Phys. A 30 (26) (2015) 1550158, http://dx.doi.org/10.1142/S0217751X15501584, arXiv:1501.02610.

[42] J. Barranco, D. Delepine, V. Gonzalez Macias, L. Lopez-Lozano, Two Higgs doublet model and leptoquarks constraints from D meson decays, J. Phys. G 43 (11) (2016) 115004, http://dx.doi.org/10.1088/0954-3899/43/11/115004.

[43] P. Bechtle, H.E. Haber, S. Heinemeyer, O. Stål, T. Stefaniak, G. Weiglein, L. Zeune, The light and heavy Higgs interpretation of the MSSM, Eur. Phys. J. C 77 (2) (2017) 67, http://dx.doi.org/10.1140/epjc/s10052-016-4584-9, arXiv:1608.00638.

[44] S. Profumo, T. Stefaniak, Alignment without decoupling: the portal to light dark matter in the MSSM, Phys. Rev. D 94 (9) (2016) 095020, http://dx.doi.org/10.1103/PhysRevD.94.095020, arXiv:1608.06945.

[45] J. Alwall, R. Frederix, S. Frixione, V. Hirschi, F. Maltoni, O. Mattelaer, H.S. Shao, T. Stelzer, P. Torrielli, M. Zaro, The automated computation of tree-level and next-to-leading order differential cross sections, and their matching to parton shower simulations, J. High Energy Phys. 07 (2014) 079, http://dx.doi.org/10.1007/JHEP07(2014)079, arXiv:1405.0301.

[46] C. Degrande, Automatic evaluation of UV and R2 terms for beyond the standard model Lagrangians: a proof-of-principle, Comput. Phys. Commun. 197 (2015) 239–262, http://dx.doi.org/10.1016/j.cpc.2015.08.015, arXiv:1406.3030.

[47] A. Alloul, N.D. Christensen, C. Degrande, C. Duhr, B. Fuks, FeynRules 2.0 — a complete toolbox for tree-level phenomenology, Comput. Phys. Commun. 185 (2014) 2250–2300, http://dx.doi.org/10.1016/j.cpc.2014.04.012, arXiv:1310.1921.

[48] T. Hahn, Generating Feynman diagrams and amplitudes with FeynArts 3, Comput. Phys. Commun. 140 (2001) 418–431, http://dx.doi.org/10.1016/S0010-4655(01)00290-9, arXiv:hep-ph/0012260.

[49] V. Hirschi, R. Frederix, S. Frixione, M.V. Garzelli, F. Maltoni, R. Pittau, Automation of one-loop QCD corrections, J. High Energy Phys. 05 (2011) 044, http://dx.doi.org/10.1007/JHEP05(2011)044, arXiv:1103.0621.

[50] G. Ossola, C.G. Papadopoulos, R. Pittau, CutTools: a program implementing the OPP reduction method to compute one-loop amplitudes, J. High Energy Phys. 03 (2008) 042, http://dx.doi.org/10.1088/1126-6708/2008/03/042, arXiv:0711.3596.

[51] P. Mastrolia, E. Mirabella, T. Peraro, Integrand reduction of one-loop scattering amplitudes through Laurent series expansion, J. High Energy Phys. 06 (2012) 095, http://dx.doi.org/10.1007/JHEP06(2012)095, arXiv:1203.0291; J. High Energy Phys. 11 (2012) 128, http://dx.doi.org/10.1007/10.1007/JHEP11(2012)128 (Erratum).

[52] T. Peraro, Ninja: automated integrand reduction via Laurent expansion for one-loop amplitudes, Comput. Phys. Commun. 185 (2014) 2771–2797, http://dx.doi.org/10.1016/j.cpc.2014.06.017, arXiv:1403.1229.

[53] V. Hirschi, T. Peraro, Tensor integrand reduction via Laurent expansion, J. High Energy Phys. 06 (2016) 060, http://dx.doi.org/10.1007/JHEP06(2016)060, arXiv:1604.01363.

[54] H.S. Shao, IREGI user manual, unpublished.

[55] F. Cascioli, P. Maierhofer, S. Pozzorini, Scattering amplitudes with open loops, Phys. Rev. Lett. 108 (2012) 111601, http://dx.doi.org/10.1103/PhysRevLett.108.111601, arXiv:1111.5206.

[56] R. Frederix, S. Frixione, F. Maltoni, T. Stelzer, Automation of next-to-leading order computations in QCD: the FKS subtraction, J. High Energy Phys. 10 (2009) 003, http://dx.doi.org/10.1088/1126-6708/2009/10/003, arXiv:0908.4272.

[57] R. Frederix, S. Frixione, A.S. Papanastasiou, S. Prestel, P. Torrielli, Off-shell single-top production at NLO matched to parton showers, J. High Energy Phys. 06 (2016) 027, http://dx.doi.org/10.1007/JHEP06(2016)027, arXiv:1603.01178.

[58] J. Butterworth, et al., PDF4LHC recommendations for LHC Run II, J. Phys. G 43 (2016) 023001, http://dx.doi.org/10.1088/0954-3899/43/2/023001, arXiv:1510.03865.

[59] R.D. Ball, et al., Parton distributions for the LHC Run II, J. High Energy Phys. 04 (2015) 040, http://dx.doi.org/10.1007/JHEP04(2015)040, arXiv:1410.8849.

[60] L.A. Harland-Lang, A.D. Martin, P. Motylinski, R.S. Thorne, Parton distributions in the LHC era: MMHT 2014 PDFs, Eur. Phys. J. C 75 (5) (2015) 204, http://dx.doi.org/10.1140/epjc/s10052-015-3397-6, arXiv:1412.3989.

[61] S. Dulat, T.-J. Hou, J. Gao, M. Guzzi, J. Huston, P. Nadolsky, J. Pumplin, C. Schmidt, D. Stump, C.P. Yuan, New parton distribution functions from a global analysis of quantum chromodynamics, Phys. Rev. D 93 (3) (2016) 033006, http://dx.doi.org/10.1103/PhysRevD.93.033006, arXiv:1506.07443.

[62] M. Czakon, D. Heymes, A. Mitov, Dynamical scales for multi-TeV top-pair production at the LHC, J. High Energy Phys. 04 (2017) 071, http://dx.doi.org/10.1007/JHEP04(2017)071, arXiv:1606.03350.

[63] A. Denner, S. Dittmaier, M. Grazzini, R.V. Harlander, R.S. Thorne, M. Spira, M. Steinhauser, Standard model input parameters for Higgs physics, https://cds.cern.ch/record/2047636, https://cds.cern.ch/record/2047636.

[64] P. Marquard, A.V. Smirnov, V.A. Smirnov, M. Steinhauser, Quark mass relations to four-loop order in perturbative QCD, Phys. Rev. Lett. 114 (14) (2015) 142002, http://dx.doi.org/10.1103/PhysRevLett.114.142002, arXiv:1502.01030.

[65] A. Denner, S. Dittmaier, M. Roth, D. Wackeroth, Predictions for all processes $e^+e^- \to$ 4fermions $+ \gamma$, Nucl. Phys. B 560 (1999) 33–65, http://dx.doi.org/10.1016/S0550-3213(99)00437-X, arXiv:hep-ph/9904472.

[66] A. Denner, S. Dittmaier, M. Roth, L.H. Wieders, Electroweak corrections to charged-current $e^+e^- \to$ 4 fermion processes: technical details and further results, Nucl. Phys. B 724 (2005) 247–294, http://dx.doi.org/10.1016/j.nuclphysb.2005.06.033, arXiv:hep-ph/0505042; Nucl. Phys. B 854 (2012) 504, http://dx.doi.org/10.1016/j.nuclphysb.2011.09.001 (Erratum).

[67] R. Frederix, Top quark induced backgrounds to Higgs production in the $WW^{(*)} \to ll\nu\nu$ decay channel at next-to-leading-order in QCD, Phys. Rev. Lett. 112 (8) (2014) 082002, http://dx.doi.org/10.1103/PhysRevLett.112.082002, arXiv:1311.4893.

[68] F. Cascioli, S. Kallweit, P. Maierhöfer, S. Pozzorini, A unified NLO description of top-pair and associated Wt production, Eur. Phys. J. C 74 (3) (2014) 2783, http://dx.doi.org/10.1140/epjc/s10052-014-2783-9, arXiv:1312.0546.

[69] M. Wiesemann, R. Frederix, S. Frixione, V. Hirschi, F. Maltoni, P. Torrielli, Higgs production in association with bottom quarks, J. High Energy Phys. 02 (2015) 132, http://dx.doi.org/10.1007/JHEP02(2015)132, arXiv:1409.5301.

[70] N. Craig, F. D'Eramo, P. Draper, S. Thomas, H. Zhang, The hunt for the rest of the Higgs bosons, J. High Energy Phys. 06 (2015) 137, http://dx.doi.org/10.1007/JHEP06(2015)137, arXiv:1504.04630.

[71] A. Denner, R.J. Guth, W. Hollik, J.H. Kuhn, The Z width in the two Higgs doublet model, Z. Phys. C 51 (1991) 695–705, http://dx.doi.org/10.1007/BF01565598.

[72] P.H. Chankowski, M. Krawczyk, J. Zochowski, Implications of the precision data for very light Higgs boson scenario in 2HDM(II), Eur. Phys. J. C 11 (1999) 661–672, http://dx.doi.org/10.1007/s100520050662, arXiv:hep-ph/9905436.

[73] D. Lopez-Val, J. Sola, Delta r in the two-Higgs-doublet model at full one loop level – and beyond, Eur. Phys. J. C 73 (2013) 2393, http://dx.doi.org/10.1140/epjc/s10052-013-2393-y, arXiv:1211.0311.

[74] T. Ježo, P. Nason, On the treatment of resonances in next-to-leading order calculations matched to a parton shower, J. High Energy Phys. 12 (2015) 065, http://dx.doi.org/10.1007/JHEP12(2015)065, arXiv:1509.09071.

[75] T. Ježo, J.M. Lindert, P. Nason, C. Oleari, S. Pozzorini, An NLO + PS generator for $t\bar{t}$ and Wt production and decay including non-resonant and interference effects, Eur. Phys. J. C 76 (12) (2016) 691, http://dx.doi.org/10.1140/epjc/s10052-016-4538-2, arXiv:1607.04538.